

Thermophoresis as a possible mechanism for aluminum oxide lobe formation

Stany GALLIER^{1,†}, Alexandre BRACONNIER^{1,2,*}, Franck GODFROY¹, Fabien HALTER², and Christian CHAUVEAU²

¹ArianeGroup, Le Bouchet Research Center, 91710 Vert-le-Petit, France

²CNRS-ICARE, University of Orléans, 45000 Orléans, France

*Present address: MBDA, Route d'Issoudun, 18020 Bourges

†Corresponding author

Abstract

This work studies the influence of the thermophoresis of fine alumina particles (“smoke”) produced during the combustion of aluminum. Direct numerical simulations of a single aluminum droplet burning in a quiescent environment suggest that thermophoresis is the main mechanism driving smoke back to the aluminum surface, hence a major contributor to the oxide lobe development. The presence of this lobe is found to distort the flow field, which favors hot and smoke-rich regions closer to the lobe, thereby enhancing thermophoresis. Parametric simulations on aluminum particle size, pressure, and oxidizer content are performed with major effects mostly from aluminum initial size. The obtained results are included in a simplified zero-dimensional model able to predict the size of the final oxide residue in good agreement with available measurements. This study supports that aluminum oxide present on the burning aluminum particle is largely due to material formed in the flame, subsequently deposited by thermophoresis.

1. Introduction

Aluminum is widely used for space and military applications since its combustion significantly enhances the performance of solid rocket motors. However aluminum combustion is complex and, despite decades of fundamental studies, is not completely understood so far. It is generally accepted that large aluminum particles (i.e. $\geq 10\text{-}20\ \mu\text{m}$) burn in the vapor-phase through a diffusion flame.¹ Combustion of aluminum produces aluminum oxide (alumina Al_2O_3) as the major product. It is predominantly present as fine particles—commonly referred to as oxide smoke with typical size $d_{ox} \approx 1\ \mu\text{m}$ —in the detached flame around the burning aluminum particle. In addition, aluminum oxide is also present on the burning particle as a distinct cap, or lobe, because liquid aluminum and its oxide are non-miscible. When aluminum is fully consumed, this lobe remains as an oxide particle, or residue. This residue can be as large as the initial aluminum particle.² The presence of an oxide lobe on the burning aluminum particle decreases the available surface for aluminum evaporation and is sometimes deemed to be responsible from the deviation from the expected d^2 law.^{1,3,4} Note that the existence of this lobe is a distinctive feature of aluminum combustion compared to liquid hydrocarbon fuels. In the field of solid rockets, oxide residues in the combustion chamber can significantly contribute to two-phase performance losses when ejected through the nozzle.⁵ Recent studies have also pointed out that the combustion of aluminum could trigger thermoacoustic instabilities in solid rocket motors^{6,7} and that the size of this oxide residue could play a significant role.

The diameter of the final oxide residue d_{res} is usually linearly related to the size of the initial aluminum particle d_{Al}^0 by $d_{res} = \beta d_{Al}^0$. The proportionality factor β has scattered values from the literature: Salita⁵ compiled various experimental results and found values in the range $0.5\text{-}0.8$. Lower values $\beta \approx 0.2$ were also attested in quench bomb measurements on aluminized solid propellants, with a strong effect of the pressurant.⁸ Similarly, experimental observations suggest that the lobe is more massive when nitrogen is used as a diluent compared to argon or helium.⁹⁻¹¹ Other experiments show that the rate of oxide accumulation grows for larger aluminum particles and lower oxygen content.¹²

A clear physical mechanism for oxide lobe formation is still missing. Some authors propose that there could be some deposition of smoke on the particle but without any further detailed mechanism.¹³⁻¹⁵ On the other hand, Dreizin¹⁰ expects this deposition of smoke to be negligible due to the strong outward flow (Stefan flow) on particle surface. He therefore advocates a diffusion of gaseous aluminum suboxides to the particle surface which could saturate an oxygen-rich phase with subsequent transformation into stoichiometric oxide. It seems also that oxide lobes are formed through material deposited from the flame rather through an internal transition.² King⁴ proposed a simplified model assuming that AIO produced in the flame diffuses back and undergoes collision-limited reaction with the surface to

THERMOPHORESIS AS A MECHANISM FOR LOBE FORMATION

form liquid Al_2O_3 . His model was applied to the combustion of a $100\ \mu\text{m}$ aluminum particle burning in a solid rocket and gave $\beta \approx 0.7$. Glorian et al.^{16,17} developed a surface reaction mechanism using ab initio computations and used it for combustion simulations of a burning aluminum droplet. They showed that oxygen-rich gaseous species diffuse to the surface, then adsorb and react to form liquid alumina Al_2O_3 on aluminum burning surface. They found that β was much dependent on particle size and nature of oxidizer and, for a $d_{Al}^0=100\ \mu\text{m}$ particle burning in air, computed $\beta=0.26$, which is significant but still lower than most experiments. This suggests that heterogeneous reactions are a possible route for alumina production directly on aluminum surface but might not be the only mechanism.

Detailed direct numerical simulations on a single burning droplet are available in the literature^{1,17–22} and they all consider that smoke produced in the flame diffuses through a Fick's law, with fume diffusion coefficients identical to gaseous species. This certainly oversimplifies the physics although it has provided reliable estimates of deposition rates.²³ The oxide lobe has been accounted for in some simulations^{18,19}—yet simplified as a spherical cap. Although the lobe seems to induce a distortion of the species/temperature profiles, there are no detailed results whether the presence of the lobe could promote smoke deposition.

In a very recent paper,²⁴ we have proposed a possible explanation based on the thermophoresis of smoke, moving back from the flame to the aluminum surface, due to intense temperature gradients. The present work is a companion paper of it, in which we propose additional parametric simulations on the effect of pressure, particle size, or oxidizer content. The objective is to complement our first results by providing a wider and more comprehensive view of the possible implications of thermophoresis on the formation of oxide lobe.

2. Experimental observations

The present study was to some extent motivated by some of our recent experimental observations conducted in our electrostatic levitator.^{9,25,26} In this set-up, a single aluminum droplet is levitated by electrostatic forces, ignited by a CO_2 laser beam, and burns in a controlled environment, allowing a large spectrum of burning conditions, such as pressure or oxidizers. High temporal and spatial resolution can be obtained, typically 40000 fps and $2.5\ \mu\text{m}/\text{pixel}$, using a high-speed camera. We do not describe the set-up in the frame of this paper and the interested reader may refer to the previously cited references.

An interesting sequence, taken from Braconnier et al.,²⁷ is presented in Fig. 1 and was obtained for a $d_{Al}=95\ \mu\text{m}$ particle burning in a $\text{CO}_2/\text{O}_2=40/60$ mixture at $p=1$ bar. Images are taken from a high-speed video and are typically separated by 0.5 ms. Image (1) is taken right after ignition and a large cloud of alumina particles is emitted and progressively evacuated by the bottom in the subsequent images. The oxide lobe—visible as a bright white spot on the aluminum particle—is clearly apparent from the beginning but may occasionally disappear as the particle rotates. A clear motion of smoke then becomes visible on the video, indicated by red arrows in image (5) *et seq.*, and this strengthens with time. The overall smoke motion is unambiguously directed towards the oxide lobe. In images (7) and (8), the motion of smoke can even be noticed in the flame at the opposite side of the lobe (small arrows), indicating a large-scale transfer across the whole flame. During this stage, the lobe grows significantly and at some point, the particle undergoes a rapid spinning in image (10).

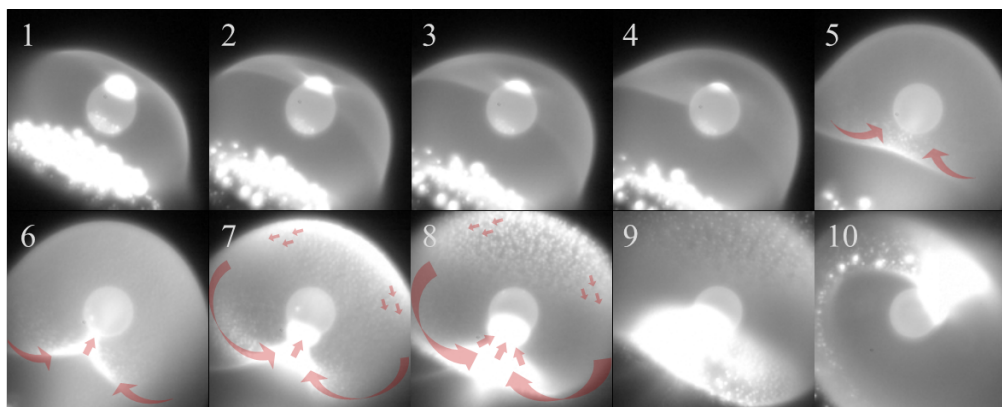


Figure 1: Sequence of a $d_{Al}=95\ \mu\text{m}$ particle burning in a $40\%\text{CO}_2/60\%\text{O}_2$ mixture at $p=1$ bar.²⁷

This observation calls for a significant motion of smoke towards the particle, mostly through the lobe. Among all experiments conducted, this behavior is not systematically noticed in such a clear manner. It seems however that it is promoted when a significant oxide lobe is present at the early stages of burning, which was often the case in CO_2 -rich environments. Nonetheless, this effect still persists in many other gases, including air.

THERMOPHORESIS AS A MECHANISM FOR LOBE FORMATION

The resulting increase in smoke concentration in the vicinity of the lobe gives rise to a brighter zone in the flame region. This led Dreizin¹⁰ to suggest the occurrence of a so-called asymmetric flame regime. We do believe that this “asymmetric” regime is actually just related to the rapid build-up of smoke above the lobe. This symmetric/asymmetric transition was studied recently by the present authors⁹ and we found that the nature of gas is of primary importance.

We end this section by a last and highly instructive sequence taken in a CO₂/O₂ mixture and presented in Fig. 2. The first images show a rather hectic ignition with many large alumina droplets dispersed in the flame. They progressively coalesce and are finally evacuated from the flame region in image (6). It seems that during those events, the oxide lobe may have been expelled as well. Thereafter, we observe a mild and steady combustion until complete burning. There is no visible lobe in the videos, nor asymmetric flame, and the particle is fully burnt out without any jetting and spinning—a rather unusual case in such environments. This unequivocally shows that when no initial lobe is present, then no lobe grows. This definitely spotlights the role of the initial lobe and possibly suggests that surface reactions during combustion are possibly too weak to induce a significant oxide production.

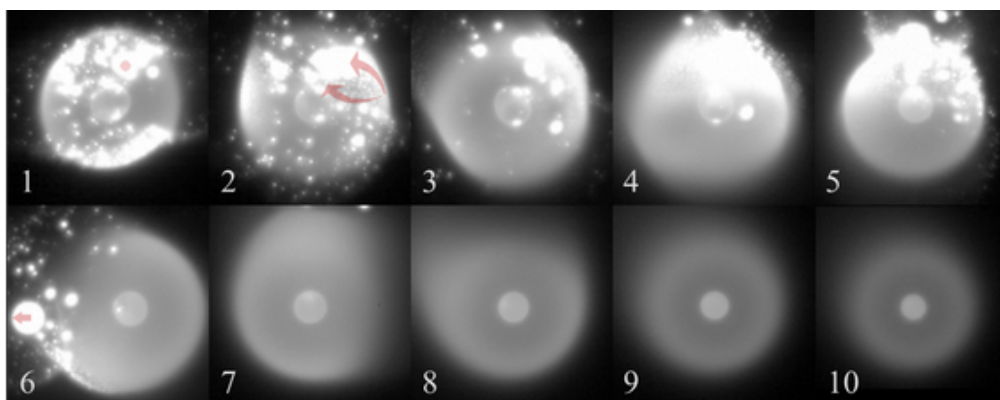


Figure 2: Sequence of a $d_{Al}=70\ \mu\text{m}$ particle burning in a 60%CO₂/40%O₂ mixture at $p=1\ \text{bar}$.²⁷

Let us here quickly summarize our observations. High-speed videos of a single burning aluminum particle support the idea that the initial presence of a lobe triggers an intense motion of smoke towards this lobe that, in turn, feeds it and makes it grow. The role of this initial lobe is substantiated by an experiment when combustion proceeds without such smoke motion when the initial lobe is missing. We are aware that more analysis is needed (including the effect of gas nature, pressure, etc.) before a definite and general conclusion can be drawn but we however believe that this puts forward a primary role of the initial oxide lobe on the underlying physical mechanism. Those observations have nevertheless fostered the following numerical works in order to provide further illumination.

3. Numerical simulations

This work considers direct numerical simulations of a single burning aluminum particle. We are interested in steady combustion—and not ignition—and we therefore assume that the thin passivating alumina layer is already molten. Aluminum droplet, as well as its oxide lobe, are assumed to be isothermal due to small Biot numbers. The flow inside the droplet is not considered and only the exterior domain (gas phase) is modeled. This work essentially focuses on micrometer-scale aluminum droplet and the Knudsen number at the aluminum droplet scale $Kn=2l/d_{Al}$ (where l is the molecular mean free path) is typically about 0.01, which legitimates considering the usual Navier-Stokes equations without any slip corrections.

3.1 Model

Accounting for spherical symmetry, the two-dimensional axisymmetric reactive Navier-Stokes equations are solved around the particle by invoking the conservation of mass, momentum, energy, and species. For brevity, equations are not recalled here and can be found in our companion paper.²⁴ Detailed transport properties are considered using standard kinetic theory and mixture laws are then used to obtain mixture viscosity, conductivity, and mass diffusivity. A perfect gas law is moreover assumed. In this work, we consider aluminum burning in oxygen-containing environments only. The reaction mechanism used for gas-phase reactions is presented in the previous reference²⁴ and includes 12 gas-phase reactions with 9 species. Gaseous Al₂O₃ is included in the mechanism as an intermediate species together with an additional fast reaction $\text{Al}_2\text{O}_3 \rightleftharpoons \text{Al}_2\text{O}_{3(l)}$ to mimic rapid condensation. In addition to this gas-phase mechanism,

THERMOPHORESIS AS A MECHANISM FOR LOBE FORMATION

an evaporation reaction is added at the surface as $\text{Al}_{(l)}=\text{Al}_{(g)}$ with rate given by a Hertz-Knudsen relation with unit sticking coefficient (see Glorian et al.¹⁷ for details). Reactive Navier-Stokes equations are solved by a finite-volume approach using our in-house code CPS and for details on the numerical strategy, the reader is referred to previously cited references.^{7,17,24}

3.2 Particle geometry and flow conditions

Computations performed in this work focus on aluminum droplets with diameters d_{Al} typical of aluminum agglomerates released during solid propellant combustion and we have investigated the following values: 100 μm , 70 μm and 40 μm . Because aluminum and its oxide are non-miscible, this binary droplet takes a specific shape as the form of two spherical caps. The exact geometry can be theoretically reconstructed based on the equilibrium of the triple line between surrounding gas, aluminum and its oxide, and depends on surface tensions. The exact solution is not displayed in the frame of this work but has been detailed in our companion paper.²⁴ We here define f_{lobe} as the mass content of aluminum oxide in this binary droplet, i.e. $f_{lobe} = m_{lobe}/m_{droplet}$ where m_{lobe} is the mass of the oxide lobe and $m_{droplet}$ the total mass of the composite droplet. Once this fraction f_{lobe} , as well as aluminum diameter d_{Al} , are prescribed, the exact shape of the binary aluminum/oxide droplet can be obtained. In this work, the investigated values of the lobe size, expressed in terms of f_{lobe} , are: 0 (i.e., no lobe), 0.1, 0.3, 0.5, 0.7, and 0.9 in order to sample across the whole lifetime of the droplet, from aluminum without lobe to the final oxide residue.

We consider quiescent conditions without any imposed flow. In that case, the position of the lobe is irrelevant. The gas domain is meshed with square elements with grid clustering close to the surface: the smallest grid spacing is about $d_{Al}/140$. The grid extends up to $25d_{Al}$ and the particle surface is discretized using approximately 100 elements. This gives a total number of grid points of about 30,000. Grid convergence was checked by considering a coarser mesh (11,000 elements) and the quantity of interest (i.e., thermophoretic flux) was off by only 3 %. Geometry is fixed in time (i.e., particle regression is not explicitly tracked) due to much longer burnback time scales compared to flow time scales. Because of small Biot numbers, we assume the particle to be isothermal: in particular, aluminum and its oxide cap share the same temperature, given by a Clausius-Clapeyron relation. Remote far-field boundary conditions are prescribed pressure p^∞ , zero gas velocity, temperature $T^\infty=300$ K and O_2/Ar mixture with various oxygen molar fraction X_{O_2} . The forthcoming simulations will consider various ambient pressures $p^\infty=1, 5, \text{ and } 10$ bar and oxidizer content $X_{\text{O}_2}=0.1, 0.2, \text{ and } 0.3$. The motivation is to evaluate to which extent pressure and gaseous environment are likely to affect thermophoresis.

3.3 Modeling oxide smoke and deposition

Liquid alumina $\text{Al}_2\text{O}_{3(l)}$ condenses as fine particles ('smoke'), which are liquid at the temperatures of interest (melting temperature of alumina is about 2330 K). The reported diameter d_{ox} of this smoke phase is typically about 1 μm .^{5,14,28} and smoke has therefore a negligible inertia (vanishing Stokes numbers). It is then considered as a passive tracer that can be followed using a mass fraction Y_{ox} given by a simple conservation equation on ρY_{ox} (with ρ the gas density). Because it is a condensed phase, it does not experience any Fickian diffusion—which is only active at the molecular scale—and there is therefore no mass diffusion term in the conservation equation of ρY_{ox} . In our previous work,²⁴ we have investigated other possible mechanisms (Brownian, diffusiophoresis, etc.) and found that only thermophoresis was likely to alter significantly the motion of such small particles. It is recalled that thermophoresis induces the displacement of suspended particles under the influence of an applied thermal gradient owing to the difference in the momentum transfer to the particle between gas molecules with a high thermal velocity and those with a low thermal velocity. Since it is proportional to the temperature gradient ∇T , thermophoresis is believed to be significant, between the detached flame and the burning aluminum surface (or the lobe), where temperature gradient is locally very large, typically $\nabla T \sim 10^7$ K/m. The thermophoretic velocity \mathbf{v}_{th} is given by²⁹ as

$$\mathbf{v}_{th} = -K_{th} \frac{\mu}{\rho} \frac{\nabla T}{T} \quad (1)$$

with

$$K_{th} = 2.294 C_c \frac{\lambda^* + 2.18 Kn}{(1 + 3.44 Kn)(1 + 2\lambda^* + 4.36 Kn)} \quad (2)$$

and the Cunningham coefficient

$$C_c = 1 + Kn(1.26 + 0.4 \exp(-1.1/Kn)) \quad (3)$$

where ρ is the gas density, μ the gas dynamic viscosity, T the temperature and λ^* the ratio between the thermal conductivity of gas and smoke particles $\lambda^* = \lambda_g/\lambda_{ox}$. A value $\lambda_{ox}=7$ W/m/K is taken for alumina at high temperatures.

THERMOPHORESIS AS A MECHANISM FOR LOBE FORMATION

In flame conditions at atmospheric pressure, the molecular mean free path l is typically about $0.5 \mu\text{m}$, so that the Knudsen number $Kn = 2l/d_{ox} \approx 1$, suggesting a transitional flow at smoke size scale. The resulting mass flux $\rho Y_{ox} \mathbf{v}_{th}$ is added to the conservation equation on ρY_{ox} in addition to the conventional flow convection term $\rho Y_{ox} \mathbf{u}$ with \mathbf{u} the gas velocity. Smoke size d_{ox} changes the thermophoretic velocity through the Knudsen number Kn in the thermophoretic constant K_{th} in Eq. (2). However, K_{th} rapidly levels off at an asymptotic value ($K_{th} \approx 0.55$) for high Kn enough (typically about 1) which is basically reached for $d_{ox}=1 \mu\text{m}$. Smaller sizes then do not lead to any further changes.

This additional thermophoretic mass flux is present within the flow but is also likely to operate between the lobe (or the aluminum surface) and the surrounding flow. The deposited mass flux j_{dep} on the lobe due to thermophoresis reads

$$j_{dep} = -\rho Y_{ox} \mathbf{v}_{th} \cdot \mathbf{n} \quad (4)$$

where \mathbf{n} is a local normal vector on the lobe pointing outwards. The total deposited mass rate \dot{m}_{lobe}^{dep} ($\text{kg}\cdot\text{s}^{-1}$) on the lobe is computed by integrating this mass flux over the lobe:

$$\dot{m}_{lobe}^{dep} = \int_{S_{lobe}} j_{dep} \cdot dS \quad (5)$$

The average deposition flux $\langle j_{dep} \rangle$ is then estimated as $\langle j_{dep} \rangle = \dot{m}_{lobe}^{dep}/S_{lobe}$ where S_{lobe} is the total surface of the oxide lobe. In each computational cell on the surface, the computed smoke mass flux $j_{dep} \cdot \mathbf{n}$ is applied as a boundary condition for the numerical flux $\rho Y_{ox} \mathbf{v}$ so as to effectively mimic an actual deposition on the particle and remove smoke from the flow. The mass rate is expressed for the lobe in Eq. (5) but can similarly be computed also for the aluminum surface.

4. Results

4.1 Mechanism of thermophoretic deposition

Figure 3 shows a map of oxide smoke mass fraction Y_{ox} for four lobe sizes, expressed in terms of oxide lobe mass fraction $f_{lobe}=0.1, 0.3, 0.5,$ and 0.7 . The burning aluminum particle is here $d_{Al}=70 \mu\text{m}$ for all cases. The spherical symmetry of the flame is clearly broken (asymmetric flame) due to the oxide lobe and this symmetry breaking is more pronounced for larger lobes. The maximum value of Y_{ox} decreases with f_{lobe} , from 0.83 ($f_{lobe}=0.1$) down to 0.66 ($f_{lobe}=0.7$), because more smoke is captured and removed from the flow.

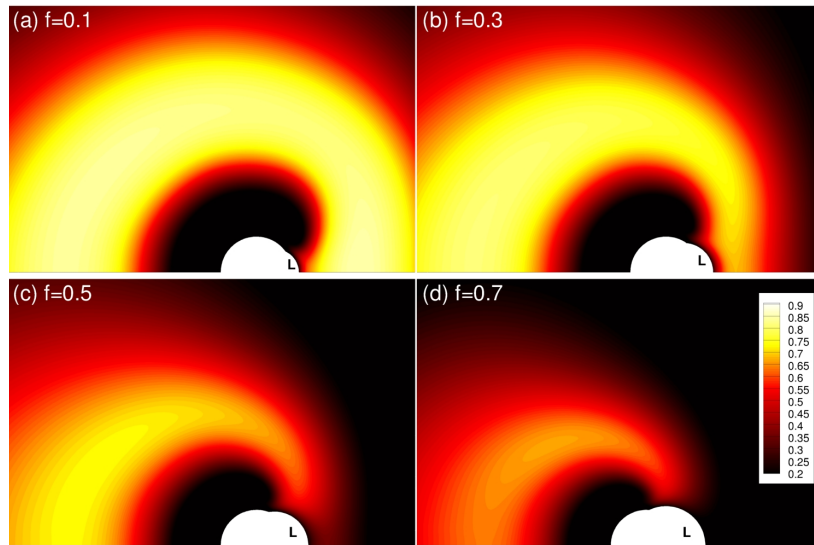


Figure 3: Oxide smoke mass fraction Y_{ox} for a $70 \mu\text{m}$ aluminum particle with different lobe size (lobe mass fraction $f_{lobe}=0.1$ (a), 0.3 (b), 0.5 (c), and 0.7 (d)). The lobe is indicated by “L”. Identical contour levels are used. Pressure is 1 bar and $X_{O_2}=0.2$.

Interestingly, the aluminum evaporation rate is found to remain almost unchanged, with only a 2 % variation. This means that aluminum combustion is not altered by the presence of the lobe, at least within our assumptions (in

THERMOPHORESIS AS A MECHANISM FOR LOBE FORMATION

particular, no heat transfer between aluminum and oxide lobe). Due to gas diffusion, there is an overall inward motion of oxidizer towards the aluminum particle, but because the lobe does not outgas, the flame is pushed back to the lobe region. The resulting higher temperature gradients and large amount of smoke hence boost an intense thermophoretic motion of nearby smoke to the lobe. The mechanism of deposition has therefore both aerodynamic (flow distortion due to the lobe) and thermophoretic origins. Since the whole droplet is supposed isothermal, the lobe has a relatively low temperature (2570 K at 1 bar) compared to the surrounding gas (about 3800 K) so that thermophoresis is much intense. The motion of the smoke is such that it follows the flame and then turns inwards, towards the lobe, exactly as in the experiments showed in Fig. 1.

Thermophoresis is operative in moving smoke back to the particle due to gradients in temperature. It is much more effective in the vicinity of the lobe first because of hot and smoke-rich regions close to the lobe, and, second, because the lobe does not release gas, so that smoke motion is not hindered. However, thermophoresis is so intense that it can even bring smoke back onto the exposed aluminum surface despite the Stefan flow due to aluminum evaporation. This can be computed by evaluating the mass rate of smoke deposited on the lobe \dot{m}_{lobe}^{dep} and the mass rate of smoke deposited directly on aluminum surface \dot{m}_{Al}^{dep} . Figure 4 shows how this mass rate ratio $\dot{m}_{lobe}^{dep}/\dot{m}_{Al}^{dep}$ changes with lobe size. When the lobe is small (low f_{lobe}), the majority of the deposited mass rate by thermophoresis is actually on the aluminum surface (since the ratio is lower than 1). As the lobe grows, most smoke deposition comes actually from the lobe and for large lobes, the deposited mass rate on the lobe is about ten times the mass rate on the aluminum surface. Similar mass rate $\dot{m}_{Al}^{dep} \sim \dot{m}_{lobe}^{dep}$ is noted for $f_{lobe} \sim 0.3$ even though in this case the lobe surface is five times smaller than aluminum surface ($S_{lobe}/S_{Al}=0.21$). This highlights the major effect of the lobe—when it is sufficiently developed—and is reminiscent of experimental observations where the smoke motion is generally clearly noted when the lobe reaches a certain size.

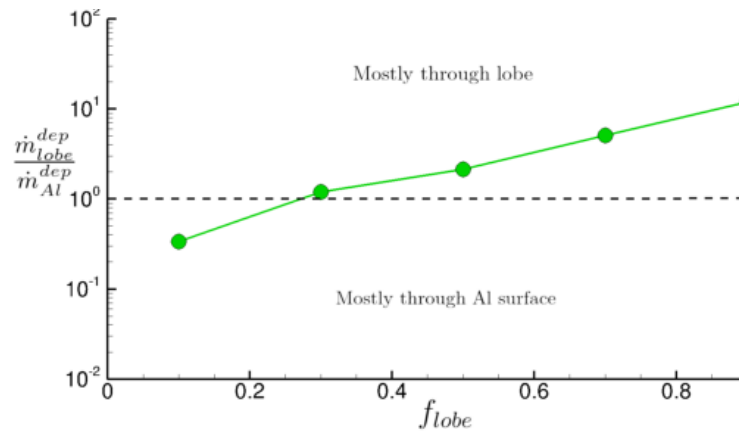


Figure 4: Ratio of deposited mass rate on lobe and aluminum surface against lobe size f_{lobe} . Case $d_{Al}=70 \mu\text{m}$, $p=1 \text{ bar}$, $X_{O_2}=0.2$.

4.2 Parametric simulations

Previous simulations have been carried out on a fixed aluminum particle size d_{Al} and at given pressure and atmosphere. Although we do not aim here at considering actual propellant gas, it is important to evaluate to which extent this strong role of thermophoresis holds for other—and more realistic—conditions. This is the case for particle size, which will alter temperature gradients, as well as pressure or oxidizer fraction that are likely to modify surface and flame temperatures. Pressure is also expected to change the molecular mean free path, hence the Knudsen number and the thermophoretic flux through K_{th} (see Eq. 2). A parametric study is hence performed on lobe size f_{lobe} , aluminum droplet diameter d_{Al} , ambient pressure p and oxygen molar fraction X_{O_2} . Investigated values are compiled in Tab. 1 and correspond to a total of 162 simulations.

A reasonable assumption is that alumina smoke deposited on the aluminum surface migrates to the lobe. Therefore, we consider the total deposition flux $\langle j_{dep} \rangle$ on the droplet by summing contributions from deposition on aluminum surface and oxide lobe. In the analysis, it is more relevant to compare this deposited mass flux relative to the mass flux of total oxide released by combustion $\langle j_{ox} \rangle$. Noting ν_{st} the mass stoichiometric coefficient of aluminum transformation to alumina ($\nu_{st}=1.89$), this comes as $\langle j_{ox} \rangle = \nu_{st} \langle j_{Al} \rangle$ where j_{Al} is the evaporated mass flux of aluminum. We therefore define the quantity f_{dep} as the fraction of deposited mass rate of alumina relative to the total alumina production as

Table 1: Values studied in the parametric study

Parameter	Values
f_{lobe}	0 – 0.1 – 0.3 – 0.5 – 0.7 – 0.9
d_{Al} (μm)	40 – 70 – 100
p (bar)	1 – 5 – 10
X_{O_2}	0.1 – 0.2 – 0.3

$$f_{dep} = \frac{\langle j_{dep}^{part} \rangle S_{Al} + \langle j_{dep}^{lobe} \rangle S_{lobe}}{v_{st} \langle j_{Al} \rangle S_{Al}} \quad (6)$$

where S_{Al} is the exposed surface of aluminum and S_{lobe} the surface of the lobe. This is an indication of the relative fraction of produced oxide that moves back to the particle. Note that if we assume f_{lobe} constant throughout the combustion, the final oxide residue size ratio β (as discussed in the introduction) would simply be

$$\beta = (v_{st} f_{dep} \rho_{Al} / \rho_{ox})^{1/3} \quad (7)$$

This shows a direct connection between this ratio f_{dep} and the final oxide residue.

4.2.1 Effect of particle size

This deposition fraction f_{dep} is presented in Fig. 5 as a function of lobe size f_{lobe} for different aluminum droplet diameters. We do observe an increase in the deposition fraction with lobe size. It is moderate for small lobes but much more marked for high f_{lobe} , typically higher than 0.6. This might be connected with the position of the smoke trail, which is now entirely above the lobe (as in Fig. 3(d))—thereby maximizing thermophoresis mass rate—and the increasing surface of the lobe. Overall, the deposition ratio is in the range 10~20 % during the early stages of combustion (i.e., small lobes) before increasing to larger values at the end of burning (large lobes).

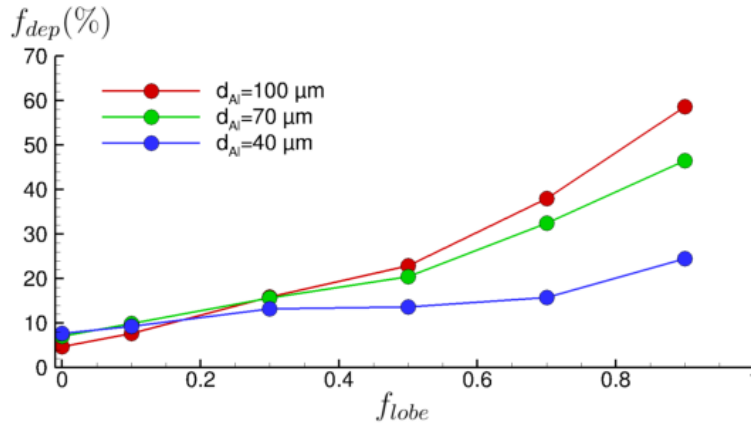


Figure 5: Deposition fraction f_{dep} as a function of lobe size f_{lobe} for different aluminum droplet sizes d_{Al} ($p=1$ bar, $X_{O_2}=0.2$).

The role of the droplet size is moderate between 100 and 70 μm but more pronounced for smaller droplets. In the case of a 40 μm aluminum droplet, thermophoresis seems weaker with a relatively constant f_{dep} . For small particles, diffusion actually becomes more intense which tends to smooth out thermal gradients. This explains why the increase in f_{lobe} seems less marked for smallest particles. An expected scenario is that thermophoresis is weak at the early stages of combustion due to small f_{lobe} then increases as the lobe grows but eventually goes down as the aluminum droplet gets smaller. Our findings are consistent with experiments by Babuk¹² showing that the rate of oxide accumulation grows for larger aluminum particles.

4.2.2 Effect of oxidizer content

In solid rocket motors, aluminum burns in a relatively lean atmosphere (small molar fraction of oxidizer), which moreover gets leaner as aluminum consumes the remaining oxidizers. Even though we here only consider O_2 environments

THERMOPHORESIS AS A MECHANISM FOR LOBE FORMATION

(more relevant oxidizers CO_2 and H_2O are left for future studies), it is instructive to evaluate to which extent oxidizer content modifies the thermophoretic deposition rate. The fraction of oxidizer does change smoke production, flame temperature T_f but also droplet surface temperature T_s (hence, lobe temperature), thus altering the local temperature gradient. Figure 6 shows the deposition fraction f_{dep} for different oxygen mole fractions. Interestingly, this deposited fraction seems relatively unaffected by oxidizer content. The deposited mass rate actually changes but similarly as the production does. In particular, low O_2 fractions induce less smoke production but also less deposition, so that the ratio is basically constant. Future works should confirm whether or not this still holds for other oxidizers such as CO_2 .

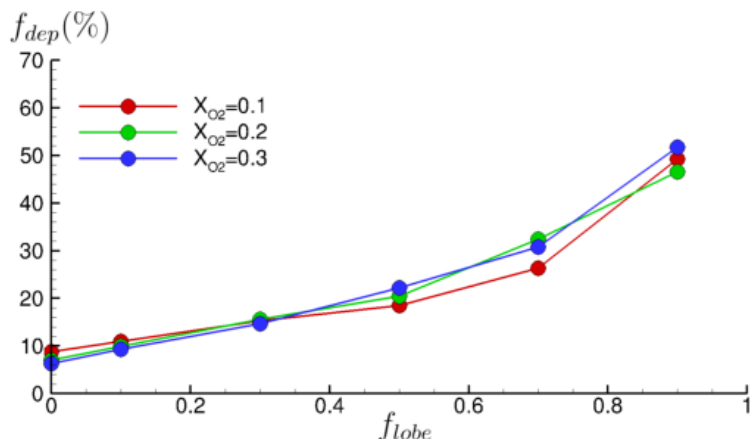


Figure 6: Deposition fraction f_{dep} as a function of lobe size f_{lobe} for different O_2 gas molar fraction ($p=1$ bar, $d_{Al}=70$ μm).

4.2.3 Effect of pressure

We finally address the role of ambient pressure which is anticipated to affect the thermophoretic motion. The molecular mean free path l indeed scales as $l \propto 1/p$, meaning that high pressures yield lower Knudsen numbers and therefore reduced thermophoretic constant K_{th} (Eq. 2). Figure 7 shows the evolution of f_{dep} for the three pressures investigated. The effect seems moderate overall. For high pressures and vanishing lobe, f_{dep} is almost zero, which means virtually no deposition in that case. But as far as the lobe grows, deposition is favored and is eventually slightly more pronounced than in the 1 bar case.

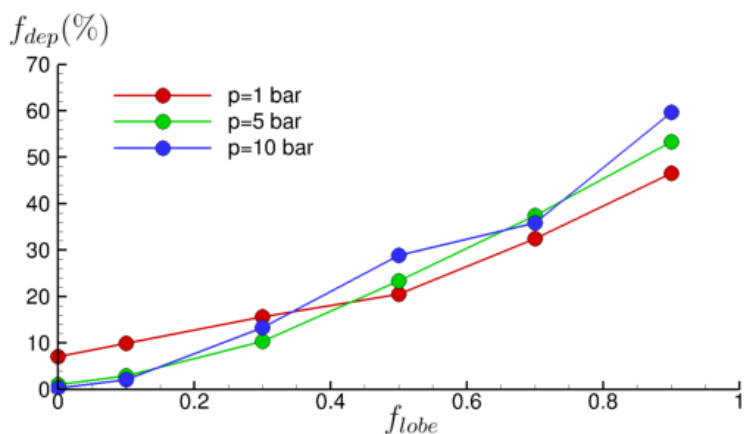


Figure 7: Deposition fraction f_{dep} as a function of lobe size f_{lobe} for different pressures ($X_{\text{O}_2}=0.2$, $d_{Al}=70$ μm).

The value of K_{th} is indeed smaller for high pressures but temperature gradients are found to increase. This is seen in Fig. 8 where a gas temperature field is shown for 1 and 10 bar. The flame temperature is clearly higher in the $p=10$ bar case compared to 1 bar (4180 K vs. 3820 K) but so is also the surface temperature (2990 K vs. 2570 K). However, temperature gradients are computed to be higher in the lobe region for $p=10$ bar. This seems supported by the temperature field of Fig. 8, which suggests that high temperature zones are much closer to the lobe. Here again, the aluminum consumption rate or the smoke production rate change with pressure, but the fraction f_{dep} of it coming back

to the surface remains relatively unaltered. This means that this quantity is relatively unaffected by ambient conditions and is mostly related to the lobe extent.

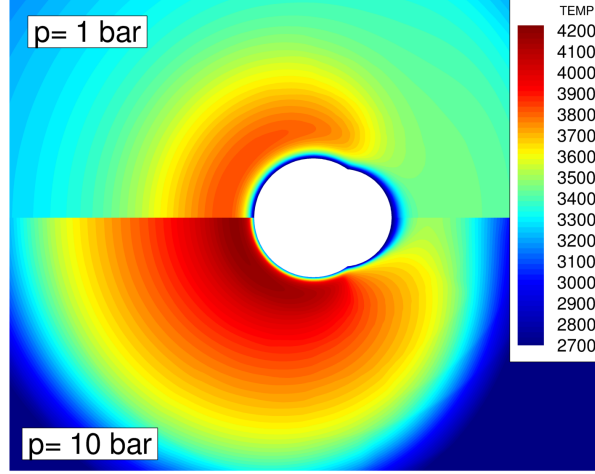


Figure 8: Temperature field around the droplet ($d_{Al}=70 \mu\text{m}$, $X_{O_2}=0.2$, $f_{lobe}=0.3$) for $p=1$ bar (top) and $p=10$ bar (bottom).

4.3 Prediction of aluminum oxide residue

Results presented heretofore can be used to propose a preliminary model able to provide some quantitative predictions of the lobe growth, hence the size of final oxide residues. Let us start with an aluminium particle of diameter d_{Al}^0 containing an initial oxide fraction f_{lobe}^0 . The evolution of aluminium V_{Al} and oxide V_{ox} volumes are then given as

$$\frac{dV_{Al}}{dt} = -\frac{\langle j_{Al} \rangle S_{Al}}{\rho_{Al}} \quad (8)$$

$$\frac{dV_{ox}}{dt} = +\frac{v_{st} f_{dep} \langle j_{Al} \rangle S_{Al}}{\rho_{ox}} \quad (9)$$

Once volumes are known—and so is f_{lobe} —all geometrical data (in particular, particle and lobe surfaces S_{Al} and S_{lobe}) can be deduced. Therefore, the model accounts for the actual exposed aluminum surface for evaporation. In order to close the model, we need to prescribe some constitutive relations for the evaporation mass flux $\langle j_{Al} \rangle$ as well as for the deposition ratio f_{dep} . When a d^2 law is assumed, the scaling $\langle j_{Al} \rangle \propto 1/d_{Al}$ is expected, which is confirmed by simulations for the range of diameters chosen. There is a slight effect of pressure and oxidizer fraction and a fitting against our simulations gives (SI units)

$$\langle j_{Al} \rangle = 2.6 \times (70 \cdot 10^{-6} / d_{Al}) \times (p/10^5)^{0.07} \times (X_{O_2}/0.2)^{0.86} \quad (10)$$

We note in passing that exponents for pressure and oxidizer fraction (0.07 and 0.86) are reminiscent of Beckstead correlation³ (respectively 0.1 and 1). Concerning f_{dep} , we have seen that it depends much on f_{lobe} and d_{Al} , while effects of pressure and oxidizer content are weak and here assumed negligible. We choose a second-order polynomial fit to model the relation $f_{dep} = F(f_{lobe})$ together with a diameter correction. The aluminum (and lobe) temperature is taken from simulations and depends on pressure and oxidizer fraction. Surface tensions or densities (ρ_{Al} and ρ_{ox}) also both depend on temperature.²⁴

Solving Eqs. (8)-(9) with prescribed functions $\langle j_{Al} \rangle$ and f_{dep} finally yields the time evolution of the burning particle and lobe growth. Figure 9 presents an example of the time evolution of the aluminum and oxide particle size with time for the combustion of a $d_{Al}^0=100 \mu\text{m}$ particle (without initial lobe) burning in three different atmospheres. Since aluminum and oxide lobe are not spheres (but sphere caps rather), we here plot a volume-equivalent diameter $d = (6V/\pi)^{1/3}$ as a more relevant parameter. Figure 9 illustrates the typical outcome of the model with the influence of pressure and oxidizer content on the burning time but also on the final oxide residue size. For those particular cases, the final residue size is typically around $50 \mu\text{m}$, leading to a size ratio $\beta \sim 0.5$. This is an encouraging result since it is in line with most experimental data, between 0.5 and 0.8, as discussed in the introduction. This supports that smoke

THERMOPHORESIS AS A MECHANISM FOR LOBE FORMATION

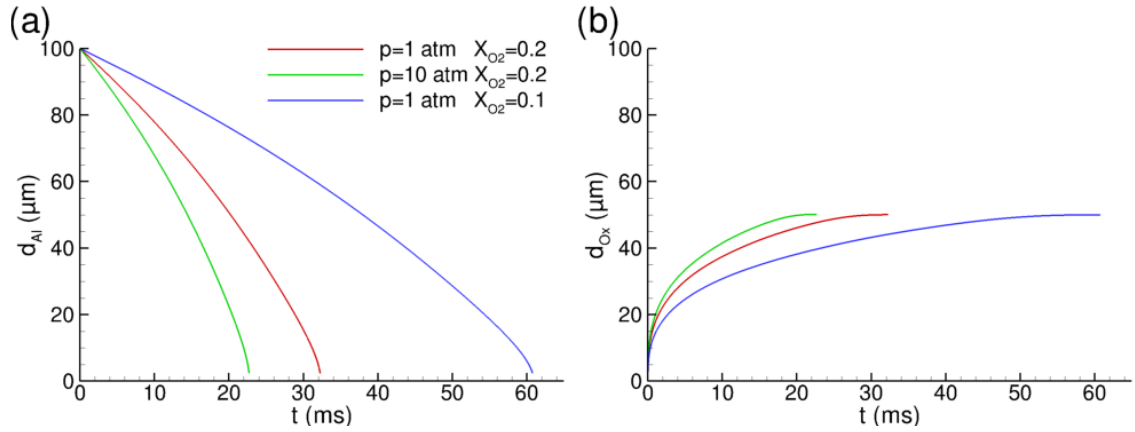


Figure 9: Predicted equivalent particle diameter for aluminum (a) and its oxide (b) for a $d_{Al}^0 = 100 \mu m$ initial aluminum droplet burning in three different atmospheres.

deposition by thermophoresis can be a dominant mechanism for lobe growth.

The effect of pressure or oxidizer content on the size ratio β was found to be negligible and the most important parameters are found to be the initial aluminum diameter d_{Al}^0 and the initial size of the lobe f_{lobe}^0 . Figure 10 shows as this size ratio β changes with initial aluminum size and initial lobe size ($p=1 \text{ bar}$, $X_{O_2}=0.2$). Large aluminum droplets lead to larger residues proportionally, with β going up to 0.7 for a $400 \mu m$ initial aluminum particle, meaning that an oxide residue of about $280 \mu m$ is expected. This effect was confirmed experimentally by Babuk¹² and is likely to explain the wide range of values of β reported in measurements, basically because β is not a constant, strictly speaking. Small particles have a β reaching a limiting value ($\beta \approx 0.42$) since diffusion acts as smoothing temperature gradients.

Another significant parameter is the initial size of the lobe f_{lobe}^0 as seen in Fig. 10(b). Large initial lobes will promote larger deposition rates at the very beginning of combustion, thus leading to a higher quantity of deposited smoke. Our experiments^{9,26} suggest that a significant lobe exists right after melting, before burning inception, probably due to oxide production on aluminum surface by heterogeneous reactions. This initial lobe is then expected to modify the amount of deposited smoke and final oxide residue as suggested by present computations.

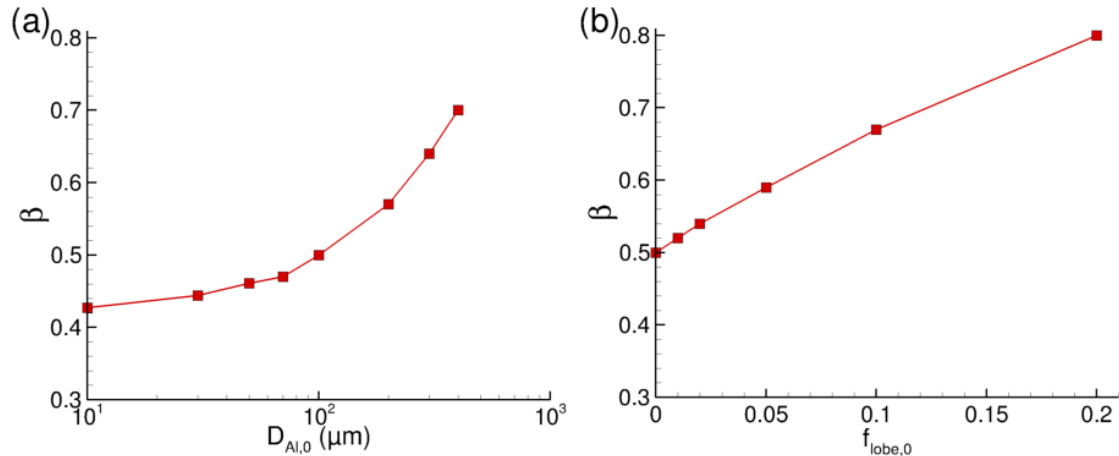


Figure 10: Oxide residue size ratio β as a function of initial aluminum size d_{Al}^0 (a) and initial lobe mass f_{lobe}^0 (b).

5. Conclusions

This work reports on direct numerical simulations of a burning aluminum droplet with a detailed geometrical representation of its oxide lobe. A major finding is that thermophoresis is predominant in driving smoke back to particle surface, thereby feeding the oxide lobe. The mechanism attested by computations is that the lobe distorts the flame, bringing hot and oxide-rich regions close to the lobe, which favors intense thermophoretic motions towards it. Paramet-

ric simulations have confirmed the lobe size and particle size to be the main quantities affecting the ratio of deposition rate to production rate, while pressure or oxidizer content have less impact. Simulation results have been processed to propose a simple zero-dimensional model, which estimates burning times and final oxide residue sizes. Final residue diameters are typically 50~80 % of the initial particle size, which is in good agreement with the scarce experimental data available. Initial particle size as well as initial lobe size—presumably produced by a heterogeneous stage prior to gas-phase burning—are found to have the most important role. Although this work strongly supports a prominent thermophoretic-based process, other aspects such as heterogeneous combustion or smoke captured by sweeping have not been considered so far and should be investigated in the future.

6. Acknowledgments

The work was funded by the French Defense Procurement Agency (DGA).

References

- [1] MW Beckstead. A summary of aluminum combustion. *RTO/NKI Special Course on Internal Aerodynamics in Solid Rocket Propulsion RTO-EN-023*, 2004.
- [2] EL Dreizin. Experimental study of stages in aluminium particle combustion in air. *Combust. Flame*, 105(4):541–556, 1996.
- [3] MW Beckstead. Correlating aluminum burning times. *Combust. Explo. Shock Waves*, 41(5):533–546, 2005.
- [4] MK King. Aluminum combustion in a solid rocket motor environment. *Proc. Combust. Inst.*, 32(2):2107–2114, 2009.
- [5] M Salita. Survey of recent al₂o₃ droplet size data in solid rocket chambers, nozzles, and plumes. *21st JANNAF Exhaust Plume Technology Meeting*, 1:1–17, 1994.
- [6] S Gallier and F Godfroy. Aluminum combustion driven instabilities in solid rocket motors. *J. Prop. Power*, 25(2):509–521, 2009.
- [7] S Gallier, B Briquet, and M Yiao. Aluminum combustion can drive instabilities in solid rocket motors: T-burner study. *J. Prop. Power*, 35(1):159–172, 2019.
- [8] S Gallier, J-G Kratz, N Quaglia, and G Fouin. Detailed analysis of a quench bomb for the study of aluminum agglomeration in solid propellants. *Prog. Propulsion Phys.*, 8:197–212, 2016.
- [9] A Braconnier, C Chauveau, F Halter, and S Gallier. Experimental investigation of the aluminum combustion in different o₂ oxidizing mixtures: Effect of the diluent gases. *Exp. Therm. Fluid Sci.*, (117), 2020.
- [10] EL Dreizin. On the mechanism of asymmetric aluminum particle combustion. *Combust. Flame*, 117(4):841–850, 1999.
- [11] A Zenin, G Kusnezov, and V Kolesnikov. Physics of aluminum particle combustion at zero-gravity. *AIAA Paper 1999-696*, 1999.
- [12] V. Babuk, V. Vasilyev, M. Belogub, and O. Romanov. Experimental study of al/al₂o₃ particle combustion in oxygen. *4th International Symposium On special topics in Chemical Propulsion, Stockholm*, 1996.
- [13] VA Babuk and VA Vasilyev. Model of aluminum agglomerate evolution in combustion products of solid rocket propellant. *J. Prop. Power*, 18(4):814–823, 2002.
- [14] VE Zarko and OG Glotov. Formation of al oxide particles in combustion of aluminized condensed systems. *Sci. Technol. Energ. Mat.*, 74(6):139–143, 2013.
- [15] JS Sabnis. Numerical simulation of distributed combustion in solid rocket motors with metalized propellant. *J. Prop. Power*, 19(1):48–55, 2003.
- [16] J Glorian, L Catoire, S Gallier, and N Cesco. Gas-surface thermochemistry and kinetics for aluminum particle combustion. *Proc. Combust. Inst.*, 35(2):2439–2446, 2015.

THERMOPHORESIS AS A MECHANISM FOR LOBE FORMATION

- [17] J Glorian, S Gallier, and L Catoire. On the role of heterogeneous reactions in aluminum combustion. *Combust. Flame*, 168:378–392, 2016.
- [18] MW Beckstead, Y Liang, and KV Pudduppakkam. Numerical simulation of single aluminum particle combustion. *Combust. Explo. Shock Waves*, 41(6):622–638, 2005.
- [19] EB Washburn, JN Trivedi, L Catoire, and MW Beckstead. The simulation of the combustion of micrometer-sized aluminum particles with steam. *Combust. Sci. Technol.*, 180(8):1502–1517, 2008.
- [20] Y Fabignon, JF Trubert, D Lambert, O Orlandi, and J Dupays. Combustion of aluminum particles in solid rocket motors. *AIAA Paper 2003-4807*, 2003.
- [21] BT Bojko, PE DesJardin, and EB Washburn. On modeling the diffusion to kinetically controlled burning limits of micron-sized aluminum particles. *Combust. Flame*, 161(12):3211–3221, 2014.
- [22] S Gallier, F Sibe, and O Orlandi. Combustion response of an aluminum droplet burning in air. *Proc. Combust. Inst.*, 33(2):1949–1956, 2011.
- [23] PE DesJardin, JD Felske, and MD Carrara. Mechanistic model for aluminum particle ignition and combustion in air. *J. Prop. Power*, 21(3):478–485, 2005.
- [24] S Gallier, A Braconnier, F Godfroy, F Halter, and C Chauveau. The role of thermophoresis on aluminum oxide lobe formation. *Combustion and Flame*, 228:142–153, 2021.
- [25] A Braconnier, C Chauveau, F Halter, and S Gallier. Detailed analysis of combustion process of a single aluminum particle in air using an improved experimental approach. *Int. J. Energ. Mat. Chem. Prop.*, 17(2):111–124, 2018.
- [26] A Braconnier, S Gallier, F Halter, and C Chauveau. Aluminum combustion in co₂-co-n₂ mixtures. *Proc. Combust. Inst.*, 38(3):4355–4363, 2021.
- [27] A. Braconnier. *Etude expérimentale de la combustion d'une particule d'aluminium isolée*. PhD thesis, University of Orléans (in French), 2020.
- [28] VA Babuk, IN Dolotkazin, and AA Glebov. Burning mechanism of aluminized solid rocket propellants based on energetic binders. *Prop. Explos. Pyrotech.*, 30(4):281–290, 2005.
- [29] L Talbot, RK Cheng, RW Schefer, and DR Willis. Thermophoresis of particles in a heated boundary layer. *J. Fluid Mech.*, 101(4):737–758, 1980.